Development of automated quantification of visceral and subcutaneous adipose tissue volumes from abdominal CT scans

Sanne D. Mensink[a], Jarich W. Spliethoff[a,b], Ruben Belder[a], Joost M. Klaase[c], Roland Bezooijen[a] and Cornelis H. Slump[b]

[a]Medisch Spectrum Twente, Dept. of Radiology, Enschede, the Netherlands;
[b]MIRA Institute for Biomedical Technology and Technical Medicine, Signals and Systems group, University of Twente, the Netherlands;
[c]Medisch Spectrum Twente, Dept. of Surgery, Enschede, the Netherlands

ABSTRACT

This contribution describes a novel algorithm for the automated quantification of visceral and subcutaneous adipose tissue volumes from abdominal CT scans of patients referred for colorectal resection. Visceral and subcutaneous adipose tissue volumes can accurately be measured with errors of 1.2 and 0.5%, respectively. Also the reproducibility of CT measurements is good; a disadvantage is the amount of radiation. In this study the diagnostic CT scans in the work - up of (colorectal) cancer were used. This implied no extra radiation. For the purpose of segmentation alone, a low dose protocol can be applied. Obesity is a well known risk factor for complications in and after surgery. Body Mass Index (BMI) is a widely accepted indicator of obesity, but it is not specific for risk assessment of colorectal surgery. We report on an automated method to quantify visceral and subcutaneous adipose tissue volumes as a basic step in a clinical research project concerning pre-operative risk assessment. The outcomes are to be correlated with the surgery results. The hypothesis is that the balance between visceral and subcutaneous adipose tissue together with the presence of calcifications in the major bloodvessels, is a predictive indicator for post - operatieve complications such as anastomotic leak. We start with four different computer simulated humanoid abdominal volumes with tissue values in the appropriate Hounsfield range at different dose levels. With satisfactory numerical results for this test, we have applied the algorithm on over a 100 patient scans and have compared results with manual segmentations by an expert for a smaller pilot group. The results are within a 5% difference. Compared to other studies reported in the literature, reliable values are obtained for visceral and subcutaneous adipose tissue areas.

Keywords: adipose tissue, segmentation, BMI, visceral - subcutaneous segmentation

1. INTRODUCTION

Obesity is a major public health problem in developed countries. Obesity is well known as a risk factor for numerous health conditions and is significantly associated with for example colorectal cancer. Colorectal cancer is the third most common form of cancer and the third leading cause of cancer-related death in the Western world.[1] Surgery remains the primary treatment, while chemotherapy and / or radiotherapy may be recommended depending on the individual patient's staging and other medical factors. Obesity is a well known risk factor for numerous health conditions, and complications after surgery. A review of Gendall et al.[2] shows evidence that obesity is a risk factor for wound infection after colorectal surgery. According to Ref.2, obesity may increase the risk of wound dehiscence, incisional site herniation, and stoma complications. Obesity is linked to anastomotic leakage, and obese patient undergoing rectal resections may be at particular risk. Operation times are longer for rectal procedures in obese patients. Prolonged procedure duration has been associated with more complications.[3] Several studies suggest obesity may not only influence the incidence of cancers but also affects the prognosis such as overall survival and disease - free survival after colorectal resection.[4,5] The Body Mass Index (BMI)

Further author information: (Send correspondence to C.H.S)
C.H.S: E-mail: c.h.slump@utwente.nl, Telephone: +31 (0)53 4892094

Medical Imaging 2011: Computer-Aided Diagnosis, edited by Ronald M. Summers, Bram van Ginneken,
Proc. of SPIE Vol. 7963, 79632Q · © 2011 SPIE · CCC code: 0277-786X/11/$18 · doi: 10.1117/12.878017

is a widely accepted indicator for obesity, however, as it divides bodyweight by height squared, it does not necessarily reflect the distribution of fat. It is well - known, *e.g.* Wajchenberg[6] that there is quite a variety between the location, visceral or subcutaneous, of the adipose tissue which may have impact on the surgical outcomes. A more accurate measure for adiposity is to compare the Visceral Adipose Tissue (VAT) area and the Subcutaneous Adipose Tissue (SAT) area and to use the so called VAT / SAT - ratio. The location of the tissue determines its metabolic profile: visceral fat is located within the abdominal wall whereas subcutaneous fat is located beneath the skin and includes fat that is located in the abdominal area beneath the skin but outside the abdominal muscle wall. Whole body CT scans are quite sufficient to study adipose tissue compartments, though MRI imaging is also successfully being used.[7–10] The aim of this project is to develop an automated software tool to detect anatomical borders and quantify the subcutaneous and visceral adipose tissue over a certain range of abdominal CT - slices. Obese patients seem to have increased pulmonary and thromboembolic risks and they also may have increased risk on a cardiovascular event. A reason of a higher complication rate could be because of a slower rate of mobilization. It is important to start the revalidation / mobilization as fast as possible after the surgery, because mobilization increases the blood supply which increases the wound healing process. This requires a change in the setup of the rehabilitation. The purpose of the present study is to provide the measurement tool for the required VAT and SAT areas / volumes, required for the quantitative assessment of the relation with surgical outcomes.[11] In the next section we describe the CT scans that we have used and the developed image analysis algorithm for the necessary image segmentation.

2. METHODS AND MATERIALS

Patients included in this project were scheduled for colorectal surgery and an abdominal diagnostic CT scan was performed. Visceral and subcutaneous adipose tissue can be accurately measured from CT - data with errors of 1.2 and 0.5 %, respectively.[6] Reproducibility of CT measurements is reported by Thaete et al.,[12] they have evaluated duplicate cross-sectional CT scans at L4 level in 16 healthy women. The correlation between duplicate measurements equals 0.99 and precision errors are reported of 1.2 % of the mean value of total adipose tissue cross-sectional area, 1.9 % for subcutaneous adipose tissue area and 3.9 % for visceral adipose area. The measurement of the total amount of fat in a CT slice of the abdomen is relatively easy because of the limited overlap between the CT - numbers or Hounsfield Units (HU) of fat and other tissues. The attenuation values for adipose tissue are -190 to -30 HU.[13] Therefore keeping the pixels within this range and disregarding the rest, gives the desired result. However, for the same reason, to distinguish between visceral and subcutaneous adipose tissue is more complicated and this requires image analysis / segmentation. This is described in the pertinent subsection. The next subsection first describes the data.

2.1 Data

To start the project, a series of CT - scans are selected from the PACS system of Medisch Spectrum Twente, Enschede, The Netherlands. Patients are included which satisfy all of the following criteria:

1. Patients with resectable colon cancer, who underwent surgery between January 9, 2008 and August 31, 2009
2. Patients with available preoperative CT scan
3. Patients with known BMI
4. Patients about whom information about complications was registered.

Because of practical limitations, 112 out of the 217 resulting CT - scans have been randomly selected and transferred in anonymous format from the PACS system. The images originate from both the institution's 64-slice MDCT (TSX-101A, Aquilion, 64, Toshiba Medical Systems Corporation, Tokyo, Japan) and the 16 Multi-Slice CT (S16 CFX, Aquilion, Toshiba Medical Systems Corporation, Tokyo, Japan) are used. The acquisition parameters are identical, *i.e.* a 1.0 mm slice thickness and a 512×512 matrix resulting in a voxelvolume slightly smaller than 1.0 mm^3; gantry rotation time 400 ms, contiguous scanning and a tube voltage of 120 kVp. The images are stored under the DICOM 3.0 protocol. The software tool was created using the numerical computing

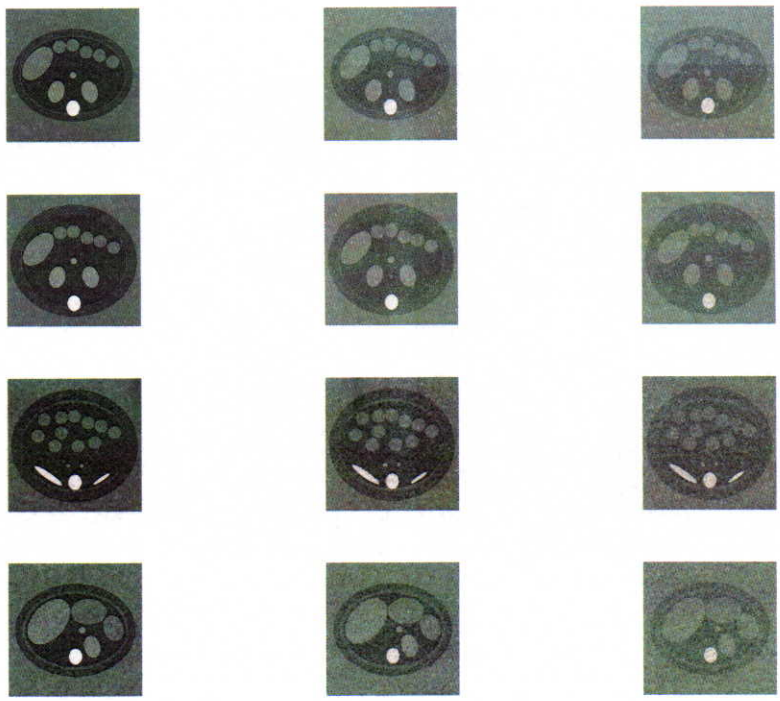

Figure 1. Four crossections are shown (column) of the four cylindrical simulated abdomens at three simulated dose levels (row). The parameters describing the phantom are presented in Table 2 through Table 5.

volume. In this study the SIAS (top of Iliac Crest) is used as anatomical reference point. A sequence of 20 slices above this point was used to calculate a patient's VAT / SAT areas and ratios. The results are summarized in Table 1 and compared with values reported in the literature.

Table 1. Comparison of results with literature.[5]

mean (sd)	Moon et al.[5]	Our results
Age	65.5 (10.5)	69.2 (9.8)
BMI	23.7 (3.2)	27.4 (5.2)
VAT / SAT - ratio	0.8 (0.4)	0.7 (0.4)
Number of patients	161	105

4. DISCUSSION AND CONCLUSIONS

We obtain satisfactory results with segmentation in 3D by a combination of image intensity ranges in Hounsfield units corresponding to adipose tissue and location dependent morphological filtering. After this we have applied the developed algorithm to a dataset of over 100 patient scans. The segmentation results are compared with the

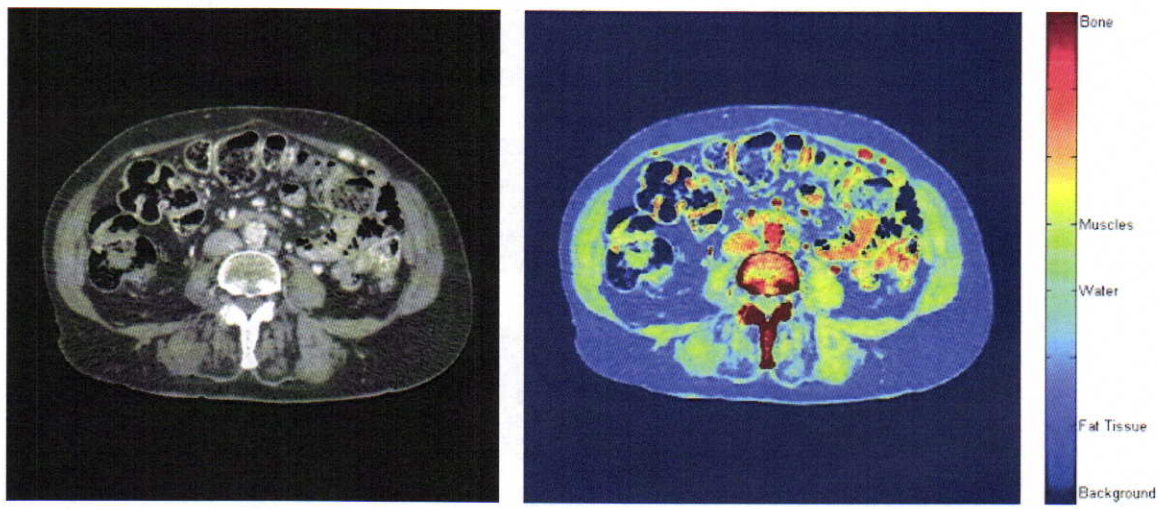

(a) Example of an abdominal CT slice.

(b) Same abdominal CT slice, now color coded, showing the attenuation values for adipose tissue (-190 to -30 HU) as light blue.

Figure 2. Original CT - slice.

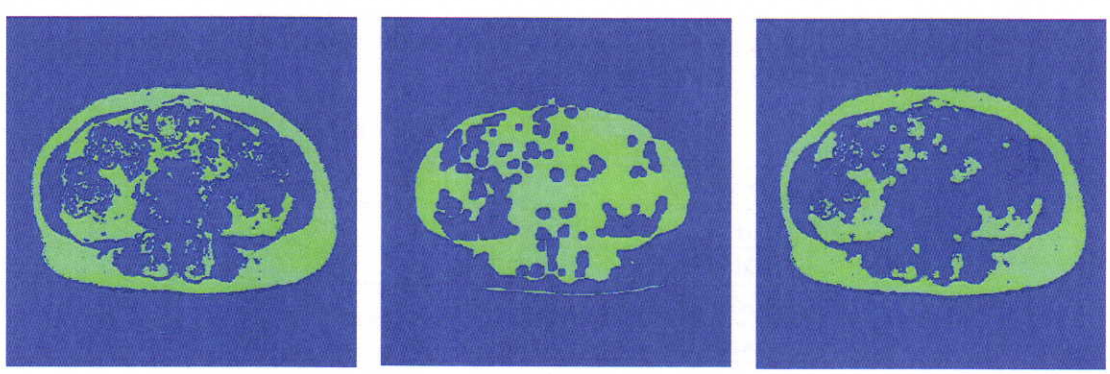

(a) Adipose tissue image

(b) Muscle tissue image

(c) Subtraction result

Figure 3. Image processing steps to select the adipose tissue and to remove muscle tissue.

environment MATLAB R7 (The Mathworks, Natick, MA). In the first phase of the project, each DICOM patient file is converted into a 3D matrix and stored locally for further processing.

2.2 Image segmentation

Image segmentation is a mature research area within the field of image analysis. Algorithms vary from simple low - level intensity based segmentations, such as histogram based methods, to highly sophisticated model based approaches of all kinds, see *e.g.*[14–16] Here we adopt simple low - level intensity based image segmentation algorithms, which we expect to be quite adequate in clinical practise. Adipose tissue can be segmented from non-adipose tissue by using an intensity threshold and manual interactions. The manual method of segmentation and quantification involves the manual tracing of the muscular body wall encapsulated in the fascia that separates the visceral adipose tissue from the subcutaneous adipose tissue, see *e.g.*,[17] which is a time - consuming task. Therefore the manual segmentation is performed on only two or three CT slices. The commonly used levels are the top of the iliac crest, the umbilicus and the level of the truncus coeliacus.[5,18] It is important to use a strict defined longitudinal level if only one scan is used to measure visceral adipose tissue. Visceral adipose tissue is usually measured at the L4-L5 vertebra interspace. While single-slice protocols provide measurements of areas expressed in square centimeters, whole-body scans provide volumetric information of adipose tissue depots. Measuring at multiple levels is expected to be more accurate since it contains information over a distribution of slices. Our purpose is to measure several slices from the ilac crest up to the truncus coeliacus. The time - consuming manual contour delineation urges for the development of automated methods. Romero et al.[19] describe a semi - automated segmentation algorithm using the umbilicus level. This reference point, however, has proven inaccurate since its position in obese subjects is fairly inconsistent. Zhao *et al.*[20] have developed an algorithm to automatically identify the body perimeter and the inner contour that separates the visceral from the subcutaneous tissue. This algorithm starts with separating the body from the image background on each slice of interest using a simple threshold. The body contour can be extracted after removal of the table object beneath the body with the help of a morphological opening operation with a circular structuring element. To extract the subcutaneous fat layer on the pertinent CT slice, radii from the outer contour are drawn at fixed 3 - degree increments towards the body center. Intensities along each radius identify the location of an inner contour point. In this way Zhao *et al.*[20] present quantitative segmentation results of 419 slices of 9 patients. Some manual correction were required in case the muscle layer on the abdominal wall appeared to be too small to be separated automatically. In Hoogenboom *et al.*[21] we have presented results of a small semi - automated pilot study (n = 10) in which a similar automated mask is generated for the detection of the subcutaneous adipose tissue, however, also requiring consistency checking and manual corrections. In this project we apply the method developed by Spliethoff,[22] which we will describe here in some detail in the next subsection.

2.2.1 Developed segmentation method

The processing steps Spliethoff[22] are described regarding the selected stack of CT images of 512 × 512 pixels as a 3D image volume. As a start, upper and lower thresholds (-190 to -30 HU)[13] are applied to select pixels within the Hounsfield attenuation range of adipose tissue. This results in the adipose volume together with the total amount of adipose tissue and reveals us the spatial location of the tissue which is used to create a subcutaneous mask bounded by the subject's skin. Subsequently a combination of morphological operations and image processing steps is applied to both the adipose volume and the abdominal wall to separate the inner part, *i.e.* the abdominal cavity, and the outer part *i.e.* the subcutaneous adipose tissue and the skin. Eventually the amount of visceral, subcutaneous adipose tissue and the sum of both is calculated and expressed in the VAT /SAT - ratio. These steps are described in more detail in the following.

In the obtained adipose volume, visceral and subcutaneous compartments are still connected at places were the abdominal wall is thin or missing. Apparently the abdominal wall is useful for further segmentation. Therefore a suitable attenuation range (-20 to 100 HU)[19] is applied to segment muscle tissue from the original selected image volume. This mask for muscle tissue is slightly dilated (dilation adds pixels to the boundaries of objects) and subsequently subtracted from the image volume. The number of pixels added or removed from the objects in an image depends on the size and shape of the structuring element (SE) used to process the image. This SE determines the precise effect of the dilation / erosion on the input image. The default SE of the algorithm is

set to respectively a 5 × 5 and a 3 × 3 matrix of ones. In an atypical situation the user can change the size of the SE to achieve a successful segmentation.

The next step is to use an external border detection algorithm to construct a binary mask of the subcutaneous adipose tissue. The body is isolated by labeling all objects in the adipose volume and the largest object is selected, assuming this is the body. A morphological operation called closing (dilation followed by erosion) is used to create a mask of the whole body. Hereafter, an edge detection is performed using the Laplacian to locate the skin. This is useful in order to reconstruct the location of the original subcutaneous adipose tissue. The final step to separate the visceral and subcutaneous compartment is a series of erosions. Although this last step completes the segmentation, also some parts of the subcutaneous adipose tissue area have disappeared due to the erosion. The generated subcutaneous mask is used to restore these parts. A series of closing and dilation operations is applied to diminish the effects of the earlier processing steps and the resulting subcutaneous and visceral adipose tissue volumes can be computed.

2.3 Simulation phantom

The method in the form as described in Ref. 22 works according to purpose, however, in about 15 - 20% of patients scans, the automated segmentation proved not successful and had to be manually corrected. This happened *e.g.* if the muscular layer of the abdominal wall was very thin or partly missing. In that case the subcutaneous boundary may leak into the abdominal cavity. The work of Spliethoff[22] continued on the groundtruth,[21] however, the fine - tuning and testing of the algorithm with the morphological processing steps appeared to be no easy task. Therefore we have designed for the current project a simulation phantom.

We have designed four different computer simulated humanoid abdominal volumes with tissue values in the appropriate Hounsfield range at different dose levels. The abdominal volumes consist of a stack of n = 20 slices with the geometrical shapes ellipsoids and cylinders, see Fig. 1. The parameters describing the phantom are presented in Table 2 through Table 5. The simulated data serves as test data for the development of adequate measurement algorithms starting with intensity based image segmentation. As expected the application of the proper Hounsfield ranges results in good segmentation results, decreasing as the noise variance increased. Using the phantom simulation we were able to optimize the settings of the segmentation method[22] and have reduced the number of required manual corrections.

3. RESULTS

The first step of the algorithm is to load the CT - data of a selected patient scan into Matlab. The user can scroll through the CT - volume and select an upper and lower slice. Matlab selects these and all intermediate slices for further processing steps. An example of an abdominal CT slice is shown in Fig. 2(a).

The gray levels in Fig. 2(a) represent the attenuation values (HU) of the various tissues, with a specific range of HU's for each tissue. Fig. 2(b) represents the same image, now a colormap is added to visualize the rough composition of the abdominal region. The attenuation values for adipose tissue are from -190 to -30 HU, and in this range is depicted as light blue in Fig. 2(b). After applying the lower and upper thresholds (-190 to -30 HU), we obtain the adipose image shown in Fig. 3(a). Applying the lower and upper attenuation range (-20 to 100 HU) to the original image in Fig. 2(a) results in the muscle tissue shown in Fig. 3(b). This muscle tissue image is slightly dilated and subsequently subtracted from the adipose image of Fig. 3(a), resulting in the image shown in Fig. 3(c). The next step is to construct a binary mask of the subcutaneous fat. For this purpose first the body in total is detected as shown in Fig. 4(a). The subsequent edge detection result is shown in Fig. 4(b). Fig. 4(c) shows the result of an erosion step. In between morphological processing steps are shown in Fig. 4(d) and Fig. 4(e), respectively. The subcutaneous mask of Fig. 4(b) is used to restore the subcutaneous parts that have eroded resulting in Fig. 4(f).

The final resulting segmentation is presented in Fig. 5. Fig. 5(a) shows the resulting total adipose tissue, while the resulting subcutaneous adipose tissue is shown in Fig. 5(b). The quantification to area and volume is by using information about the scales of pixels, which can be retrieved from the metadata of the DICOM files from the CT scanner. Because we know which pixels represent the total fat volume and the subcutaneous fat volume, we can easily determine the amount of visceral fat by subtracting the subcutaneous fat from the total fat

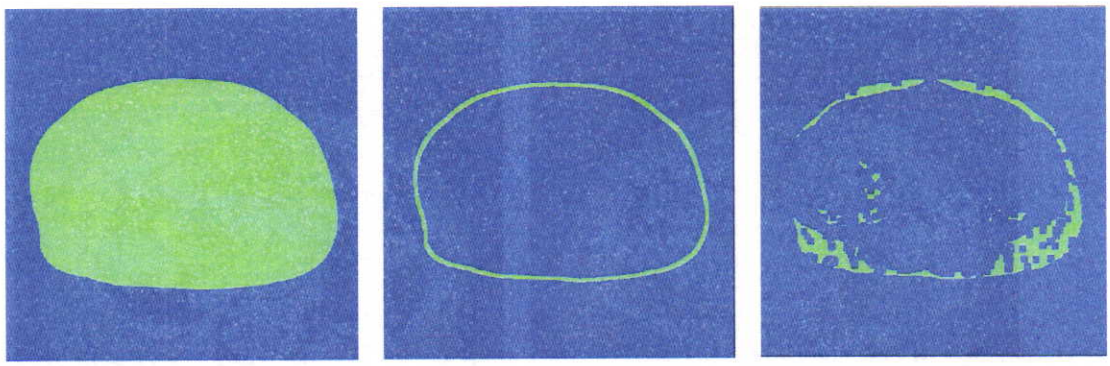

(a) Body mask image (b) Subcutaneous mask image (c) Result erosion step

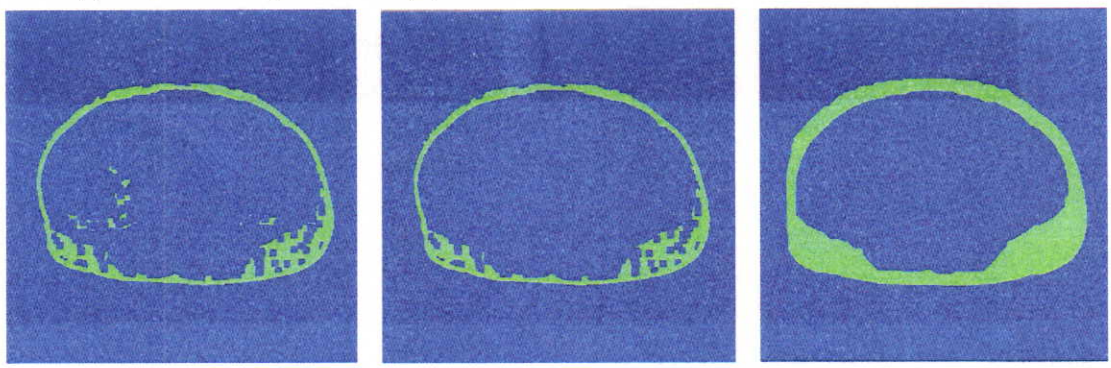

(d) In between morphological step (e) In between morphological step (f) Subcutaneous result

Figure 4. Image processing steps and morphological operations to obtain the subcutaneous adipose tissue.

results of a previous small pilot study including manual segmentations by an expert.[21] These results are within a 5% difference. Compared to other studies reported in the literature, reliable values are obtained for visceral and subcutaneous adipose tissue areas. The algorithm as described in[22] is in error segmenting the visceral adipose tissue, see for example Fig. 6, in cases where the muscular layer of the abdominal wall was very thin or partly missing. Such a situation is depicted in Fig. 7(b).

With fine-tuning and testing of the algorithm on the numerical phantom, we have been able to reduce the number of miss classifications considerable. We now estimate that in less than 3 % of the scans manual interaction is still required. An example of the final result of the improved algorithm is shown in Fig. 8 for the same CT - slices as in Fig. 6 and Fig. 7.

APPENDIX A. DESCRIPTION SIMULATION PHANTOM

In order to develop, test and validate the segmentation algorithm, four numerical test phantoms are designed. The numerical phantoms each consist of a stack of 20 slices. The slices are are composed of various ellipses with help of the MATLAB algorithm *phantom*, which generates also the well - known Shepp - Logan phantom which is widely used for testing reconstruction algorithms. The generated matrices are 512 $\times$ 512 pixels which corresponds for coordinates (x, y) with a range from -1 to +1. The details about the composition of the four numerical simulation phantoms are comprised in Table 2 through Table 5. In these four tables, each row describes an ellipse; the first column contains the Hounsfield number of the pertinent ellipse, if ellipses overlap the resulting Hounsfield number is added. The second and third columns are the length of the horizontal and vertical semiaxis, respectively. The fourth and fifth column are the center coordinates and the sixth column is the angle between the two semiaxis.

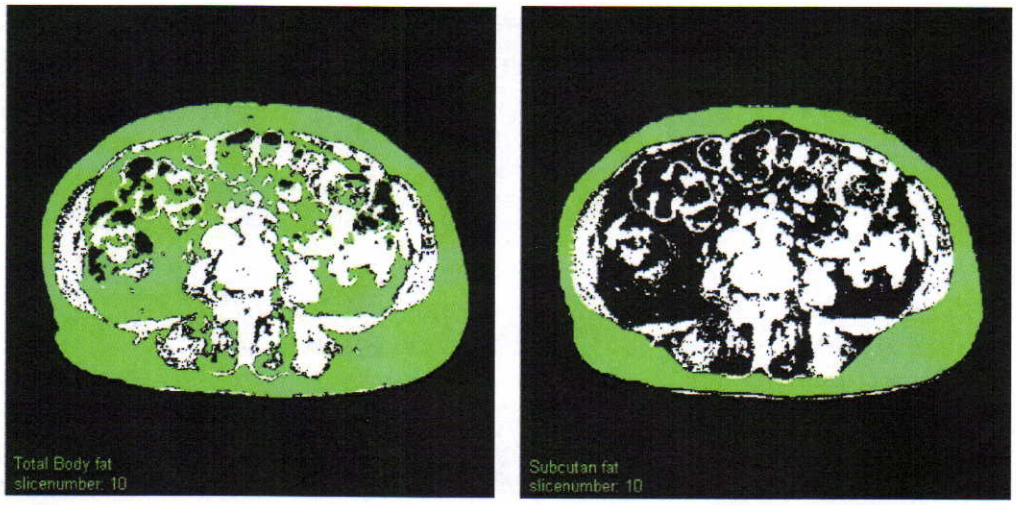

(a) Resulting total adipose tissue image (b) Resulting subcutaneous adipose tissue image

Figure 5. Resulting segmentation.

Figure 6. Example of miss classification of the visceral adipose tissue due to leakage of the subcutaneous estimation due to a small or missing muscular layer on the abdominal wall.

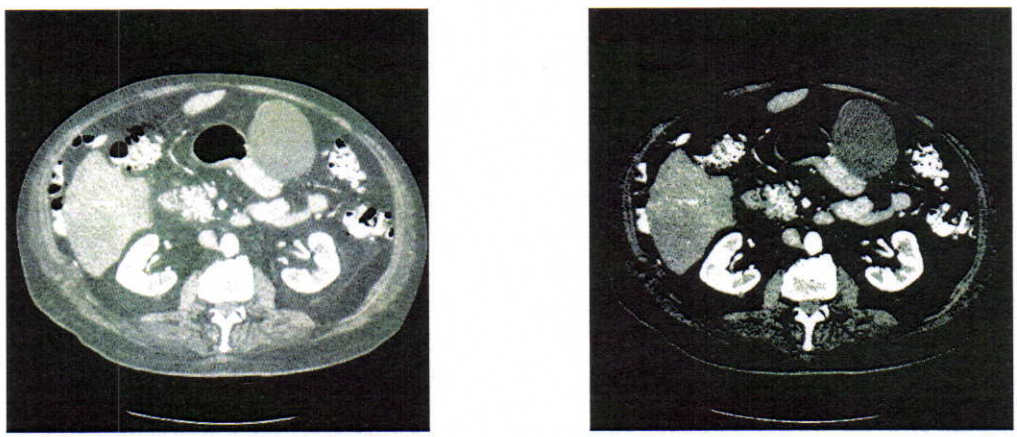

(a) Original of the misclassified slice (b) Missing muscles at the abdominal wall

Figure 7. Original CT - slice.

Figure 8. For the same slices as in Fig. 6 and Fig. 7 the result of the segmentation.

Table 2. Description of the first numerical simulation phantom, consisting of 13 ellipses.

A	a	b	x_0	y_0	ϕ
-100	0.9	0.7	0	0	0
50	0.8	0.6	0	0	0
-70	0.78	0.58	0	0	0
600	0.1	0.12	0	-0.5	0
200	0.12	0.17	0.25	-0.25	15
200	0.12	0.17	-0.25	-0.25	345
160	0.3	0.17	-0.53	0.18	50
220	0.05	0.05	0	0	0
125	0.1	0.1	-0.2	0.43	0
125	0.1	0.1	0	0.45	0
125	0.1	0.1	0.2	0.35	0
125	0.1	0.1	0.4	0.30	0
125	0.1	0.1	0.6	0.20	0

Table 3. Description of the second simulation phantom, consisting of 13 ellipses.

A	a	b	x_0	y_0	ϕ
-100	0.95	0.85	0	0	0
50	0.8	0.7	0	0	0
-70	0.78	0.698	0	0	0
600	0.1	0.12	0	-0.65	0
200	0.12	0.17	0.25	-0.25	15
200	0.12	0.17	-0.25	-0.25	345
160	0.3	0.17	-0.53	0.18	50
220	0.05	0.05	0	0	0
125	0.1	0.1	-0.2	0.43	0
125	0.1	0.1	0	0.45	0
125	0.1	0.1	0.2	0.35	0
125	0.1	0.1	0.4	0.30	0
125	0.1	0.1	0.6	0.20	0

By adding white zero - mean Gaussian noise with standard deviations equal to 20, 50 and 80, respectively, we obtain the 12 test phantoms depicted in Fig. 1.

REFERENCES

[1] World Health Organization, "(http://www.who.int/mediacentre/factsheets/fs297/en/)," (2006).

[2] Gendall, K., Raniga, S., Kennedy, R., and Frizelle, F., "The impact of obesity on outcome after major colorectal surgery," *Dis. Colun Rectum* **50**, 2223–2237 (2007).

Table 4. Description of the third simulation phantom, consisting of 19 ellipses.

A	a	b	x_0	y_0	ϕ
-100	0.95	0.85	0	0	0
50	0.8	0.7	0	0	0
-70	0.795	0.65	0	0	0
600	0.1	0.12	0	-0.55	0
600	0.25	0.05	-0.4	-0.45	325
600	0.15	0.03	0.4	-0.5	35
220	0.03	0.03	-0.1	-0.3	0
220	0.03	0.03	0.1	-0.3	0
125	0.1	0.1	-0.55	0.15	0
125	0.1	0.1	-0.3	0	0
125	0.1	0.1	0.05	0	0
125	0.1	0.1	0.3	0.05	0
125	0.1	0.1	-0.2	0.43	0
125	0.1	0.1	0	0.45	0
125	0.1	0.1	0.2	0.35	0
125	0.1	0.1	0.4	0.3	0
125	0.1	0.1	0.6	0.2	0
125	0.1	0.1	-0.45	0.4	0
125	0.1	0.1	-0.2	0.2	0

Table 5. Description of the fourth simulation phantom, consisting of 9 ellipses.

A	a	b	x_0	y_0	ϕ
-100	0.9	0.7	0	0	0
50	0.8	0.6	0	0	0
-70	0.75	0.55	0	0	0
600	0.1	0.12	0	-0.4	0
200	0.12	0.17	0.25	-0.25	15
160	0.4	0.25	-0.4	0.13	50
220	0.05	0.05	0.1	0	0
125	0.27	0.2	0.2	0.28	0
130	0.15	0.2	0.57	0.03	200

[3] Blee, T., Belzer, G., and Lambert, P., "Obesity: is there an increase in perioperative complications in those undergoing elective colon and rectal resection for carcinoma?," *Am. Surg.* **68**, 163–166 (2002).

[4] Calle, E., Rodriguez, C., and Thurmond, K. W., "Overweight, obesity, and mortality from cancer in a prospectively studied cohort of U.S. adults," *N. Engl. J. Med.* **348**, 1625–1638 (2003).

[5] Moon, H., Joo, Y., Jeong, C., Jung, E., Lee, Y., Hong, S., Ha, W., Park, S., and Choi, S., "Visceral obesity

may affect oncologic outcome in patients with colorectal cancer," *Annals of Surgical Oncology* **15**, 1918–1922 (2008).

[6] Wajchenberg, B., "Subcutaneous and visceral tissue adipose tissue: their relation to the metabolic syndrome," *Endocrine reviews* **21**, 697–738 (2000).

[7] Ross, R., Léger, L., Morris, D., de Guise, J., and Guardo, R., "Quantification of adipose tissue by MRI: relationship with anthropometric variables," *J. Appl. Physiol.* **72**, 787–795 (1992).

[8] Abate, N., Burns, D., Peshock, R., Garg, A., and Grundy, S., "Estimation of adipose tissue mass by magnetic resonance imaging: validation against dissection in human cadavers," *J. Lipid Research* **35**, 1490–1496 (1994).

[9] Ludescher, B., Machann, J., Eschweiler, G., Vanhofen, S., Maenz, C., Thamer, C., Claussen, C., and Schick, F., "Correlation of fat distribution in whole body MRI with generally used anthropometric data," *Invest. Radiol.* **44**, 712–719 (2009).

[10] Jin, Y., Imielinska, C., Laine, A., Udupa, J., Shen, W., and Heymsfield, S., "Segmentation and evaluation of adipose tissue from whole body MRI scans," in [*MICCAI 2003*], Ellis, R. and Peters, T., eds., *LNCS* **2878**, 635–642 (2003).

[11] Mensink, S., "BMI, visceraal en totaal vetvolume in relatie tot het ontstaan van postoperatieve complicaties bij patienten met een colorectale maligniteit," *Stage maart - augustus, Radiologie, Medisch Spectrum Twente, Enschede* (2010).

[12] Thaete, F., Colberg, S., Burke, T., and Kelly, D., "Reproducibility of computed tomography measurement of visceral adipose tissue area," *Int. J. Obes.* **19**, 464–467 (1995).

[13] Yoon, D., Moon, J., Kim, H., Choi, C., Chang, S., Yun, E., and Seo, Y., "Comparison of low - dose CT and MR for measurement of intra - abdominal adipose tissue," *Acad. Radiol.* **15**, 62–70 (2008).

[14] Xu, C., Pham, D., and Prince, J., "Medical Image Segmentation Using Deformable Models," in [*Handbook of Medical Imaging, vol. 2 Medical Image Processing and Analysis*], Fitzpatrick, J. and Sonka, M., eds., 129 – 174, SPIE Press, Bellingham, WA (2000).

[15] Suri, J., Wilson, D., and Laxminarayan, S., "Handbook of Biomedical Image Analysis, vol I: Segmentation Models, part A," in [*Topics in Biomedical Engineering*], Tzanakou, E. M., ed., Kluwer Academic, Dordrecht (2000).

[16] Suri, J., Wilson, D., and Laxminarayan, S., "Handbook of Biomedical Image Analysis, vol II: Segmentation Models, part B," in [*Topics in Biomedical Engineering*], Tzanakou, E. M., ed., Kluwer Academic, Dordrecht (2000).

[17] Yoshizumi, T., Nakamura, T., Yamane, M., Islam, A. H. M. W., Menju, M., Yamasaki, K., Arai, T., Kotani, K., Funahashi, T., Yamashita, S., and Matsuzawa, Y., "Abdominal fat: standardized technique for measurement at CT," *Radiology* **211**, 283–286 (1999).

[18] Tokunaga, M., Hiki, N., and Fukunaga, T., "Effect of individual fat areas on early surgical outcomes after open gasterectomy for gastric cancer," *Br. J. Surg.* **96**, 496–500 (2009).

[19] Romero, D., Ramirez, J., and Marmol, A., "Quantification of subcutaneous and visceral adipose tissue using CT," in [*International Workshop on Medical Measurement and Applications: Benevento, Italy, 2021 April*], *MeMea*, 123–133 (2006).

[20] Zhao, B., Colville, J., Kalaigian, J., Curran, S., Jiang, L., Kijewski, P., and Schwartz, L., "Automated quantification of body fat distribution on volumetric computed tomography," *J. Comput. Assist. Tomogr.* **30**, 777–783 (2006).

[21] Hoogenboom, M., Klaase, J., Belder, R., Bezooijen, R., and Slump, C., "Measurement of visceral and subcutaneous adipose tissue," in [*Proceedings of the 4th annual symposium of the IEEE - EMBS Benelux Chapter, 9-10 November 2009, Twente, The Netherlands*], Veltink, P., ed., 1–4 (2009).

[22] Spliethoff, J., "Development of a matlab tool for 3D quantificaton of subcutaneous and visceral adipose tissue using CT," *Institute of Technical Medicine, Faculty of Science and Technology, University of Twente, In association with Department of Surgery, Medisch Spectrum Twente, The Netherlands* (2009).